

# Unsupervised Behaviour Analysis of News Consumption in Turkish Media

Didem Makarođlu<sup>a,b,\*</sup>, Altan Cakir<sup>c,d</sup> and Behçet Uđur Töreyn<sup>b</sup>

<sup>a</sup>*Demirören Teknoloji A.S., İstanbul, Turkey*

<sup>b</sup>*Signal Processing for Computational Intelligence Group, Informatics Institute, Istanbul Technical University, Istanbul, Turkey*

<sup>c</sup>*Physics Engineering, Faculty of Science and Letters, Istanbul Technical University, Istanbul, Turkey*

<sup>d</sup>*Istanbul Technical University Artificial Intelligence, Data Science Research and Application Center, Istanbul, Turkey*

## ARTICLE INFO

**Keywords:**

Clickstream

Social Media

Ensemble Clustering

Digital Media Industry

## ABSTRACT

Clickstream data, which come with a massive volume generated by human activities on websites, have become a prominent feature for identifying readers' characteristics by newsrooms after the digitization of news outlets. It is essential to have elastic architectures to process the streaming data, particularly for unprecedented traffic, enabling conducting more comprehensive analyses, such as recommending mostly related articles to readers. Although the nature of clickstream data has a similar logic within websites, it has inherent limitations to recognize human behaviours when looking from a broad perspective, which brings the need to limit the problem in niche areas. This study investigates the anonymized readers' click activities on the organizations' websites to identify news consumption patterns following referrals from Twitter, who incidentally reach but propensity is mainly routed news content. The investigation is widened to a broad perspective by linking the log data with news content to enrich the insights rather than sticking into the web journey. Methodologies for ensemble cluster analysis with mixed-type embedding strategies are applied and compared to find similar reader groups and interests independent of time. Various internal validation perspectives are used to determine the optimality of the quality of clusters, where the Calinski Harabasz Index (CHI) is found to give a generalizable result. Our findings demonstrate that clustering a mixed-type dataset approaches the optimal internal validation scores, which we define to discriminate the clusters and algorithms considering applied strategies, when embedded by Uniform Manifold Approximation and Projection (UMAP) and using a consensus function as a key to access the most applicable hyper parameter configurations in the given ensemble rather than using consensus function results directly. Evaluation of the resulting clusters highlights specific clusters repeatedly present in the separated monthly samples by Adjusted Mutual Information scores greater than 0.5, which provide insights to the news organizations and overcome the degradation of the modelling behaviours due to the change in the interest over time.

## 1. Introduction

In recent years, news readership behaviours have shifted towards online channels after the digitization of news organizations and the rise of social media (Flaxman et al., 2016), which has a growing effect on consuming news. The importance of acknowledging the trend of news sources has been aroused by news outlets that need to generate new revenue to adapt and survive in this era. Relatedly, the cruciality of intermediaries has been recognized, and early studies have focused on identifying the effects of these sources on attracting and holding consumers' attention by guiding users to new content (Benlian, 2015; Chiou and Tucker, 2017; Dellarcas et al., 2013). Recent studies have shown that reaching news content through social and nonsocial channels shows different patterns (Möller et al., 2020), how news reader behaviours are formed with social (Facebook) and nonsocial media channel referrals at an aggregated level (Bar-Gill et al., 2021), and how readers spend time on the website and have the propensity to share the news differentiated by

the referral channels (Köster et al., 2021). As a microservice, Twitter has become a key player in social media and is used more than on average across 37 countries for reading, sharing, and discussing news in Turkey (Yanatma, 2018). Strongly preferred as disseminating the news, Twitter also mediates access to pages of news outlets. Considering that each social media site has different page structures, dynamics, and methods of influencing users, it is necessary to examine them separately to analyse the readers directed from these channels to news outlets. To the best of our knowledge, using Twitter as a social referring channel in identifying the behavioural patterns of the readers directed to the news organizations' websites by clicking on news links on Twitter, have yet to be studied. In this paper, we delve into uncovering referred users' behaviour by clustering methodologies. However, readers tend to navigate away from social media and direct towards news websites with broad and diverse interests and intentions, making it difficult to cluster for long periods. Therefore, we hypothesized and experimentally showed that working with separated datasets in this multidimensional environment is advantageous in recognizing and generalizing user patterns. By providing the distribution of the news category interest breakdowns of individual and general behaviours over time, we found that the behaviours diverge over months; hence, working monthly

\*Corresponding author

✉ didem.makaroglu@demirorenteknoloji.com (D. Makarođlu);

makaroglu17@itu.edu.tr (D. Makarođlu); altan.cakir@itu.edu.tr (A.

Cakir); toreyn@itu.edu.tr (B.U. Töreyn)

ORCID(S): 0000-0001-9960-2113 (D. Makarođlu); 0000-0002-8627-7689 (A. Cakir); 0000-0003-4406-2783 (B.U. Töreyn)

arXiv:2202.02056v2 [cs.SI] 8 Oct 2022

datasets is beneficial in diminishing the volume and increasing the correlation within the samples.

## 2. Research Setting

The investigated datasets belong to *Hürriyet*, a news organization located in Turkey, founded in 1948 and is active not only on its website since 2004 but also promotes the contents and live broadcast in its social media accounts. In our one-year period of analysis, between April 2019 and March 2020, the website had approximately 150 M unique users and 300 M visits per month. The traffic from the reference sites can be grouped as Social (Facebook, Twitter, Instagram, LinkedIn, YouTube) and Nonsocial (Organic, referred by Google, other), with monthly visit shares of 8% and 92%, respectively, and Twitter has 25% of all social referrals. The objective of this study is to analyse referral users' behaviour; thus, within this scope, our datasets include clickstream data, which are collected from the organization's website, and news content data. We limit our study with the collected data to uncover unsupervised behaviours of the referred users' patterns without comparing the findings with the nonsocial referrals, so this study measures neither the contribution of social referral users' behaviour and news consumption on the website nor the causal effect of being directed to the news outlets (Mao and Zhang, 2015). This work presents a comprehensive methodology of ensemble clustering and includes different kinds of embedding as input (i.e., UMAP) after experimenting with different sampling strategies (i.e., random, stratify). Our method evaluates performance metrics with clustering techniques to ensure that behavioural clusters are stable and optimal within this structure. Furthermore, we provide a validation process to measure the similarity of the ensemble clustering with the optimal results. We evaluate the clusters generated by the selected clustering method over twelve months and show the behavioural patterns' stability and consistency in specific clusters.

The rest of the paper is organized as follows and can be followed from Figure 1, which illustrates the framework of our system. Section 3 provides a discussion about related research on clickstream analysis and modelling, clustering with input data-types. Section 4 presents our dataset, including the collection and processing data platform and the analysis of the distributions. Section 5 describes the methodologies utilized in this work, including sampling and embedding strategies, ensemble clustering evaluation and comparisons, and discusses successful clustering. Finally, Section 6 concludes the article and presents our future work.

## 3. Related Literature

Clickstream data have been used to identify web usage and characteristics in many contexts (Catledge and Pitkow, 1995; Castellano et al., 2013). Clustering techniques have been studied to utilize hidden user behaviours (Su and Chen, 2015; Wang et al., 2013; Grech and Clough, 2016a) and related to this approach, unsupervised techniques have been

established to predict future groups (Zhang and Kamps, 2010). To identify the dominant behaviour groups, social networks and time-based frameworks are proposed (Lin et al., 2014) and enriched by having similarities to the group behaviour and individual propensities (Zheng et al., 2013). As news readers have been studied in various approaches, recently, the research focus shifted to differentiating news consumption by considering the effects of referral channels (Möller et al., 2020; Köster et al., 2021) and intermediaries' power on the algorithmic level (Thorson and Wells, 2016; Wells and Thorson, 2017). In our study, we also aim to find unsupervised readership behaviours on the news outlets for the specific referral channel Twitter by using ensemble clustering methodologies without having neither ground truth nor predefined patterns in the data (Wang et al., 2016; Bogaard et al., 2019a).

As an unsupervised approach, for clustering user behaviours, there are different techniques, including centroid-based (K-means, K-Medoids) (Arora et al., 2016), hierarchy-based (Agglomerative) and density-based (DBSCAN (Schubert et al., 2017), HDBSCAN (McInnes et al., 2017)) partitions. These algorithms have some advantages and disadvantages when considering various factors, such as scalability, time and space complexity, the ability to deal with categorical and numerical data types, noise and outliers. These algorithms need predefined values, including  $k$  numbers (K-means, BIRCH, Gaussian Mixture), the epsilon value, the minimum number of points (DBSCAN, HDBSCAN), and linkage metrics including average, single, complete, or ward (Agglomerative). In recent years, artificial neural networks have also been used for unsupervised clustering methods by applying autoencoders. One method is harnessed a deep autoencoder architecture (McConville et al., 2021) we refer to as N2d, which takes advantage of deep neural networks to represent lower-dimensional data. With this method, after learning autoencoder embedding representations, UMAP (McInnes et al., 2020) is applied to better clustering with lower dimensions using local manifold learning. Similar to other clustering algorithms, this algorithm needs parameter optimization during model training and after reducing dimensions to form better clusters.

Ensemble methods have been proposed to overcome the limitations of clustering algorithms when used individually. The main purpose of these methods is to combine algorithms with relative deficiencies with appropriate methods and to apply various dataset features or points with higher accuracy rates in a way that can capture the relationship between them. In the first step, called library generation, the aim is to obtain the set of  $m$ -many clustering algorithms,  $K = \{K_1, K_2, ..K_m\}$ , where  $K$  represents the set of clustering algorithms, and  $K_i$  represents each clustering algorithm with different set of parameters, and  $i=1, ..., m$ . It is revealed that the greater the clustering algorithms in this method focus on various and different features, the greater they can improve the contents of the clusters to be obtained by combining them at the consensus stage (Kuncheva and Vetrov, 2006). Thus, ensembling over a set of differences rather than

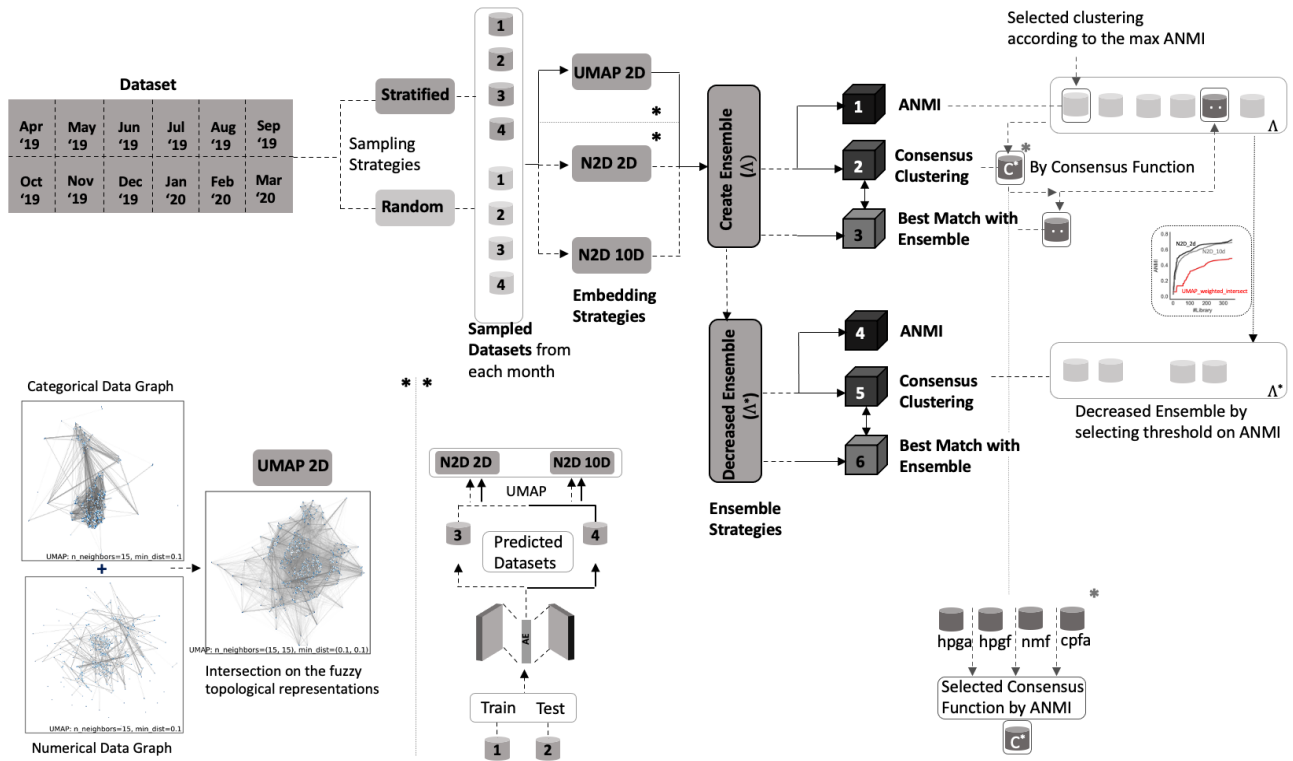


**Figure 1:** Methodology architecture. N2d embedding strategies preparation is shown at the bottom-left corner. With the N2d embedding approach, the 1<sup>st</sup> and 2<sup>nd</sup> samples are predicted by training on the 3<sup>rd</sup> and 4<sup>th</sup> samples. UMAP 2D is prepared by intersecting categorical and numerical feature graphs as illustrated at the bottom-left corner for one sampled dataset. The ANMI values are calculated for each consensus function result and then selected with the maximum value, shown at the bottom-right corner.

similar labels will yield more efficient results. The K-means algorithm is generally preferred in the library generation step because of its scalability and low complexity (Fern and Lin, 2008; Azimi and Fern, 2009; Alizadeh et al., 2014; Akbari et al., 2015; Pividori et al., 2016; Yang et al., 2017). Among the methods used in this step are obtaining results with different starting points or different numbers of clusters with a single algorithm, working on samples with different data points or features, obtaining results on the same data points and features with more than one algorithm or combining several methods. In the consensus step, the  $K^*$  clustering algorithm, which will be used as the primary clustering method, is obtained from the cluster ensembles within the set of  $K$  by integrating results of the clustering with the consensus function. These functions are grouped under four main categories by (Boongoen and Iam-On, 2018) and can be listed as follows: direct, feature-based, pairwise similarity-based, and graph-based approaches.

To compare the performance of the clustering algorithms that are used in the consensus step, in this study, we inspired by a previous work (Helfmann et al., 2018), where new clusters are generated by consensus functions from predefined parameter space and compared accordingly. The algorithm procedure is described in Algorithm 1. The first strategy obtains the consensus by averaged normalized mutual information (ANMI) maximization. The second strat-

egy consists of two steps. First, the algorithm generates clusters by a consensus function and then finds the labels in the ensemble that share the most information with the consensus step by the maximum normalized mutual information (NMI). It was shown that the optimal hyperparameters found in the second strategy give at least the fitted result as consensus clustering  $K^*$ . Instead of a precise consensus function, in the last step, we applied methods including the cluster-based similarity partitioning algorithm (CSPA) (Strehl and Ghosh, 2002), the hypergraph partitioning algorithm (HGPA) (Strehl and Ghosh, 2002), the hybrid bipartite graph formulation (HBGF) (Fern and Brodley, 2004) and NMF-based (nonnegative matrix factorization) consensus clusterings (Li et al., 2007)) and then selected the one that has the maximum AAMI score (see A.1). Although we have an ensemble of consensus function results, only the HPGA and NMF methods resulted with the highest AAMI, and among these, the HPGA method was 95% more voted.

## 4. Observational Data Analysis

### 4.1. Design and Processing of Data Platform

Clickstream datasets are collected for the research period (April 2019 - May 2020) (Fig. 2) through web browsers by using Amazon Web Services (AWS; Elastic Beanstalk, Kinesis Data Streams, Kinesis Firehose, API Gateway, Lambda, S3, Redshift, EC2) technologies (Varia et al.,

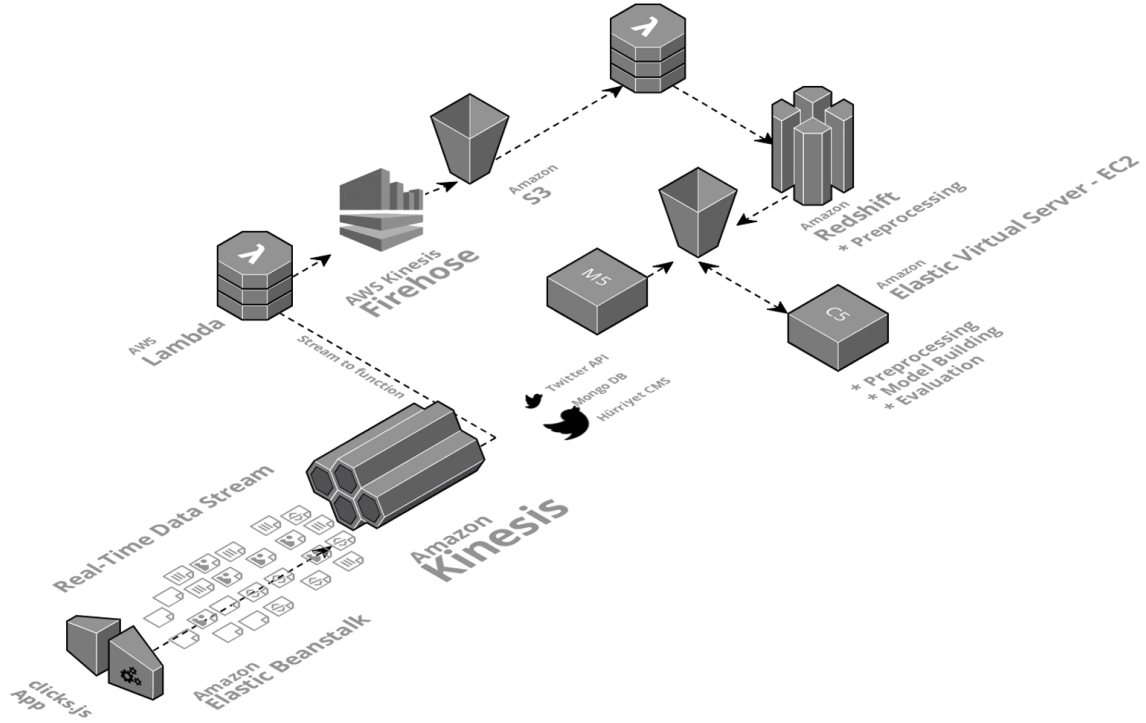


**Figure 2:** Clickstream data collection and preprocessing architecture on AWS (Varia et al., 2014). The clickstream data, generated by the readers’ navigation actions on the website, and mainly the consecutive HTTP requests from a single IP address, are collected in the S3 buckets following the pipeline (from left to right): Hürriyet clicks.js application (collects each visit’s action as a request from the website) → Elastic Beanstalk (scaled up to 20 virtual machines to meet traffic load) → Kinesis Data Streams (scaled up to 30 shards) → Lambda (to separate actions by referral types) → Kinesis Firehose → S3 → Lambda → Redshift (to provide large-scale query). The datasets are prepared on Redshift by querying and saved to S3 buckets. News content-based datasets (from Mongo DB) and additional sources are also collected on the S3 storage by EC2 virtual machines. Further analyses are processed on the EC2 virtual machines with instance type between C5.2xlarge to c5.4xlarge by reaching S3 buckets.

---

#### Algorithm 1: Hyperparameter search

---

**Data:** Data  $D = \{x_1, x_2, \dots, x_n\}$  to cluster; Set  $K$  of ensemble clustering algorithms; Set  $T$  of consensus clustering algorithms

**Result:** Matched hyperparameter configuration with the selected consensus clustering

**for**  $k \in K$  **do**

Find the clustering results  $C(k)$  with the given clustering algorithm  $k$  for the investigated dataset;

Produce consensus clustering results from the given  $T$ ;

$t^{AAMI} = \operatorname{argmax}_{t \in T} AAMI(C(t), T)$ : Find the AAMI result of consensus clustering from produced clustering based on  $T$ .

**return**  $k^* = \operatorname{argmax}_{k \in K} AAMI(C(k), t^{AAMI})$

---

2014), which have been actively managed by the company, to enable elastic processing and storage for high-volume data. The collected real-time streaming data are combined and processed on Redshift and then stored on the S3 buckets, which can be accessed through both EC2 virtual machines and local environments. Content-based information

collected and combined individually from the company’s servers and AWS.

**Clickstream Data**, stored in separated log files with a total size of 20 TB of sequentially semistructured format data for one year, belong to the visitors’ site history. An identification number (ID) is generated for each anonymized visit on the website, and the data span these visits’ navigation, including actions related to reading, time, browsing platform, content and location. The dataset is aggregated to each visit level such that a single entrance contains all articles read and content-based information included. As stated in previous research (Makaroğlu et al., 2019), the distribution of total hourly visits referred from Twitter is similar to the hourly distribution patterns within Twitter when considering Hürriyet keywords. Therefore, we deduce that the breakdowns of time-dependent distribution can shed light on the microservice usage patterns; with this inference, timestamps are expanded as *Hour*, *Week*, *dayoftheWeek*. The number of distinct articles accessed in a visit is represented as *VisitDepth* (the total number of contents), rather than embedding as sequential data. Twitter referrals are filtered from each visit’s referring channel, and the rest of the data are excluded. The category of the articles is represented as categorical names, e.g., travel, magazine, and sports. Only *LeadCategory* (see Section 4.2) is used during the analysis

steps. The columnist names of the articles also included in a single dimension.

**Content-Based Data** spans additional information about articles read by the visitors during the research, including *Postingduration* (number of days between the date content is published on the website and the date of the visit), *NamedEntityRecognition(NER)* results (Aras et al., 2021), *Person, Location, Organization*, and the daily *Contentsuccess* rank. Daily success ranks are calculated by scaling daily articles' Pageview (PV) scores within their category from 1 (lowest) to 100 (highest). We limit named entities according to the highest TFxIDF (Term Frequency x Inverse Document Frequency) scores within the scope of this study. The missing values in the categorical data types are not imputed; instead, they are represented in the dataset as *unknown : UNK*.

After all the processing, the dataset contains 5,666,125 visits originating from Twitter generated by 2,261,164 unique visitors, and includes the dimension as follows: *Hour, Week Number, Week Name, Month, Location (City, Country), Device (Mobile, PC), Visit Depth, Content Success, Posting Duration, LeadCategory, Columnist, NamedEntityRecognition (NER\_P(Person), NER\_O(Organization), NER\_L(Location))*.

#### 4.2. Analysis of LeadCategory Distribution

The first article accessed in the referred visit of the streaming data has a prominent role in leading readers from the social media environment and has a directed news consumption with more completion rates (Bar-Gill et al., 2021). Early studies showed that the interests in the news topics change over time (Liu et al., 2010a). We thus examine the lead categories' patterns by several breakdowns to show to what extent the distributions change, including browsing platform (to measure the effects of device preferences (Xu et al., 2014)), location and compare them with the general reading distributions over months. As described in Section 4.1, each article's category information is included in the clickstream data with predefined topics  $C = \{c_1, c_2, \dots, c_n\}$ , where  $c_i$  represents the topics e.g. 'Current Affairs', 'Sports'. Category-level interests are formulated by dividing total number of clicks,  $N = \{N_1, N_2, \dots, N_n\}$  of each category topic ( $c_i$ ) with total clicks  $N_{total}$  made by user ( $u$ ) within the investigated month ( $m$ ) such that the outputs are given as the following distribution vectors:

$$T(u, m) = \left( \frac{N_1}{N_{total}}, \frac{N_2}{N_{total}}, \dots, \frac{N_n}{N_{total}} \right), \quad N_{total} = \sum_i^m N_i, \quad (1)$$

where  $N_i$  is the total number of pageviews that the user made on the referred articles that are classified as the specific category, ( $c_i$ ), and  $N_{total}$  is the total number of clicks that the user made for the given month. These distributions are found by considering individual anonymized user *IDs*' as well as the *Overall* group of monthly readers. However, the referral *IDs* vanished quickly for each breakdown

(Figure 3). A possible explanation for the observed differences in the rates of enjoyment is that the readers can systematically clear the *IDs*. To rule out this possibility, rather than tracking the individuals, we grouped them within discrete time windows, such that in case the referral *ID* shows up in one month, its group is defined as  $1^{st}$ , if it is in two months, then the group is defined as  $2^{nd}$ , until the  $11^{th}$  entrance in 1 year. Relatedly, all monthly user distributions are computed by dividing one year into 12 months and comparing divergence by grouping successor months as  $1^{st}, 2^{nd}, \dots, 11^{th}$ . The Jensen–Shannon Divergence (JSD) metric (see Appendix A.1) is used to measure similarity with the given distributions. We obtain category-based characteristics by averaging each group's JSD value. Figure 3 and 4 depict that the lead category interests are differentiated across the grouped months and show that the overall month distribution is more constant than that of individuals in all three breakdowns, including Mobile, PC(Desktop), and City.

## 5. Methodology

This study utilizes an ensemble clustering evaluation method for patterns based on features extracted from readership browsing and content-based data. In Section 5.1, we explore different combinations of two embeddings as input representations (i.e., UMAP, N2d). In Section 5.2, we discuss the sampling approaches and evaluation of the selection of the minimum sample size. In Section 5.3, we experimentally investigate ensemble clustering methodologies and evaluate the optimal clustering methods. In Section 5.4, we discuss the results of the conducted experiments for the interpretation of reader behaviour stability that we obtained.

### 5.1. Embedding High Dimensions

When the correlation of categorical and numerical features before proceeding to the clustering step is below a specific value, the success in this step is affected, as it can eliminate the redundant information during clustering. When we examined the correlation in all data types (numerical, categorical, ordinal), we observed that it changes within the limits of 0.2 to 0.75 over the months. Therefore, before proceeding to the clustering step, it is confirmed that none of the correlations found surpass the maximum cut-off of 0.75. One hot encoding is applied for categorical data, and power transformation is applied for numeric data types. To make the numerical values more Gaussian-like, in this step, Yeo-Johnson's transform (Yeo and Johnson, 2000) is applied, which supports both positive and negative values and makes the data zero-mean while minimizing skewness. After the encoding step, we experiment with two embedding representations named uniform manifold approximation and projection (UMAP) (McInnes et al., 2020) and N2d (McConville et al., 2021).

UMAP uses a graph-based approach to project the high-dimensional space to the lower dimension while preserving the global structure. The  $L_2$  norm for numeric values and the Dice distance for categorical data types were used as distance criteria. As stated in the paper, with this method,

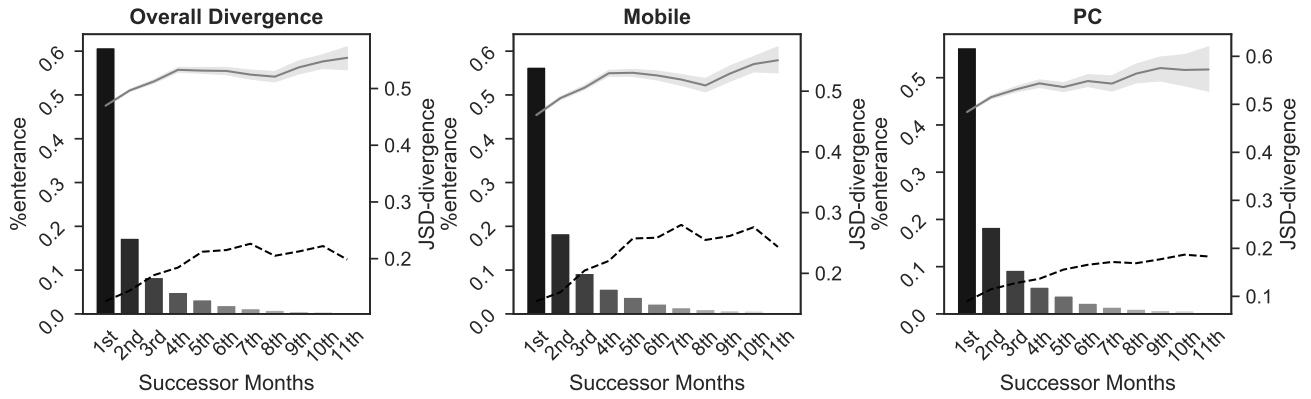


**Figure 3:** Comparison of lead category distribution by overall month (dashed black) and device types, including PC and mobile (grey). The X-axis represents the group level of entrances. The left Y-axis represents the rate of entrances within all datasets, and the right Y-axis shows the average of JSD values corresponding to the given groups.

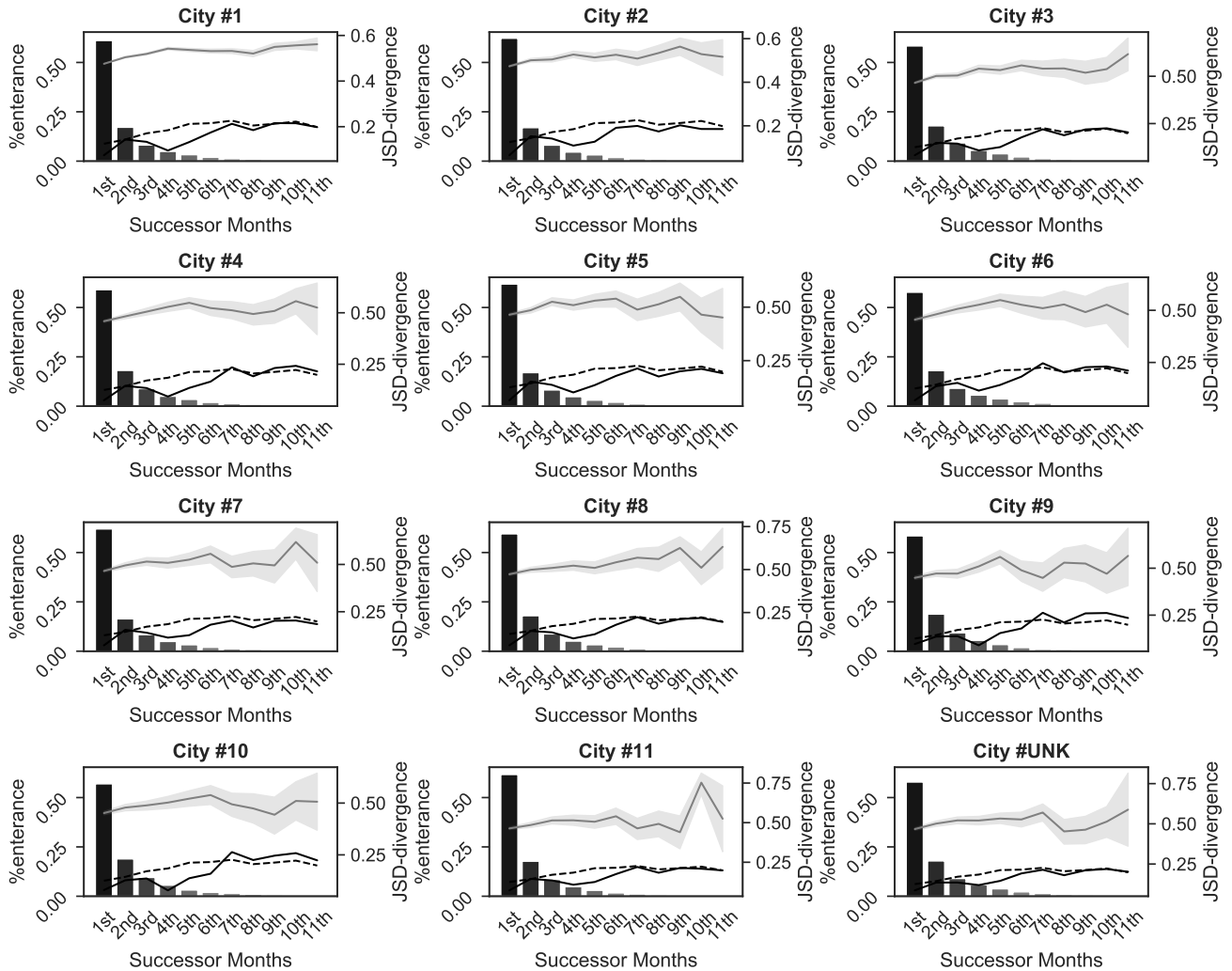


**Figure 4:** Comparison of city-level lead category distribution by overall month (dashed black), city-level month (black) and individuals (grey). The X-axis represents the group level of entrances. The left Y-axis represents the rate of entrances within all datasets considering the investigated cities, and the right Y-axis shows the average of JSD values corresponding to the groups. The # numbers represent the different cities, which are positioned in descending order according to the total number of entries they have made during one year.

we can generate fuzzy simplicial sets independently. UMAP supports intersecting two graphs and then embedding them as a consensus graph in low-dimensional space to create a single fuzzy simplicial set. The intersected graph neither has mostly dense areas as in categorical representation nor is weakly connected, as in the numerical graph. Instead, it has the middle range of all connectivity placed by the probability of edge existence. To achieve this unity, we used percentages of categorical columns as weight parameters.

N2d lowers the dimensions by creating autoencoders with a trained neural network. After having a dense layer of created autoencoders, this method adds manifold learning to increase clusterability performance by preserving local structures and capturing global structures. The article (McConville et al., 2021) states that if the total number of clusters in the dataset is known beforehand, the size in the UMAP stage should be defined accordingly. In this approach, we compared the 10 dimensions used in the original article to represent 10 known clusters and the 2-dimensional UMAP results after learning the autoencoders that we used in the first method as the final representation dimension of the dataset. Since our target is having clustering  $C = F_C(F_M(F_A))$ , with a better represented embedding space applied on dataset  $D$  with  $n$  data points in  $d$  dimensions  $D = \{x_1, x_2, \dots, x_n\} \subseteq R^d$  in this approach, we are searching for the most applicable clustering algorithm ( $F_C$ ), after having a manifold learner ( $F_M$ ) of the autoencoder ( $F_A$ ).

## 5.2. Sampling Approach

Most of the clustering algorithms' complexity is related to the number of sample data points. Therefore, it is both efficient and necessary to work on small-sized samples that can accurately represent the data, especially when working with large datasets. For this purpose, based on the results we obtained in Section 4.2, where we observed that the interests of the users change over time by the news category, we select samples from each month to keep correlations among news interests as well as to include current news events that took place in that month and correlated with each other. Stratified sampling is an approved sampling strategy that captures the main characteristics from the given dataset, is profoundly applied in large-scale datasets, and gives high accuracy when sampled from the features (Jing et al., 2015). We compared different sampling strategies within the same months to observe the minimum sample size that we could proceed with, including monthly behaviours. Therefore, on the samples that we selected both at random and stratified by news categories from each month, the K-means algorithm is used to evaluate the internal validation of the clusters, which is scalable and can return fast results. Silhouette coefficient (SI) (Rousseeuw, 1987), Calinski Harabasz index (CHI) (Caliński and Harabasz, 1974), Davies Bouldin scores (DB) and Dunn index-type (DI) (Dunn, 1974) measurements were compared by evaluating the number of clusters between 2 and 30 on four random and four stratified samples that we obtained from 5000 to 30000 in increments

of 1000 data points. To evaluate the clustering tendency of each sample, the Hopkins test (Banerjee and Dave, 2004) is applied to the sampled datasets, which gave values close to 1 for highly clusterable data. According to the result of this test, if the values are close to 0.5, it is concluded that the data are uniformly distributed, and therefore, clusterability is not possible. This value is found to be above 0.95 for all sample sizes for the given months, and as the sample size is increased, its clusterability also increases. Although the results of UMAP give lower values than the N2d approaches, especially for certain months, its clusterability is within the range of acceptable values that remain above 0.95.

### 5.2.1. Evaluation of sampling by internal metric validations

To evaluate the approach that the subsets of sampling strategies are related to each other, the similarity of each validation with the other results in its group is investigated. The adjusted mutual information (AMI) (Vinh et al., 2010) (See Appendix A.1) score is computed during this evaluation because it could measure the success of the groups' association, regardless of the order of the labels and the sample size. An overview of this process can be found in Algorithm 2. First, the metric scores correspond to the  $k$  values calculated concerning the selected sample size range in each month's random and stratified sampling strategies. After that, they were binned with the Freedman-Diaconis rule (Freedman and Diaconis, 1981). While binning, each sampling strategy is evaluated between its minimum and maximum values in its primary group as random and stratified, so the results of different approaches are not suppressed by each other. After the metric results are binned and labelled, AMI scores are calculated. To compare the validation information that a sample size shares with the sample group, the Averaged Adjusted Mutual Information (AAMI), which has proven success in ensemble methods (Strehl and Ghosh, 2002; Helfmann et al., 2018), is computed.

One of the stratified sampling results from November is shown in Figure 5. Except for CHI, the AAMI values remained relatively stable even when the sample size was increased, which we expected to observe to set the minimum sample size. Even though we used internal validity scores to determine the sample size, considering only the distance of the data points intra- or inter-clusters may cause nonconvex geometries not to be detected, or this approach might not be meaningful for the cluster centres that are embedded in nonlinear sub manifolds (Helfmann et al., 2018). The fact that any label cannot be known beforehand due to unsupervised learning problems confirms that we cannot use the external validity index in this problem where we aim to cluster user behaviours. For these reasons, we performed a knowledge-based assessment to confirm the stability of the resulting cluster in Section 5.4.3.

## 5.3. Methodology of Ensemble Clustering

We applied a method from a previous study (Helfmann et al., 2018) and referred to Strategy 1 and our approach to Strategy 2, which is shown in the model architecture in

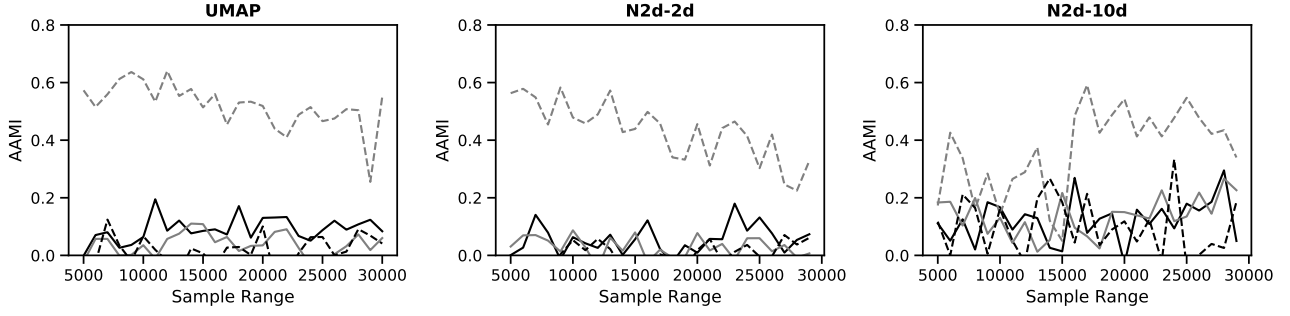


**Figure 5:** UMAP-2d, N2d-2d, and N2d-10d obtain AAMI test results according to sample sizes. The colours in the graph lines represent applied internal validation metrics that are SI, DB, DI, and CH given in black, grey, dashed black, and dashed grey, respectively. One of the stratified samplings of November is selected for representation purposes. The X-axis represents the sample sizes increasing from 5000 to 30000. The y-axis of the grid picture represents the AAMI values.

---

**Algorithm 2:** Search of sample size
 

---

**Data:** Set  $K$  of cluster sizes; Set  $M$  of internal validation metrics; data  $D = \{x_1, x_2, \dots, x_n\}$  to cluster; investigated sample range  $S$

**Result:** AAMI of each sample size for the evaluated metric

**forall**  $s \in S, m \in M, k \in K$  **do**

Find internal validation score for each metric  $m$  in the set of  $M$  correspond to the cluster size of  $k$  in the set of  $K$ , for selected  $s$  in the set of  $S$  ;  
 Scale the results between  $[0,1]$  within the given internal validation metric  $m$  ;  
 Bin the scaled results by FD rule within the given  $m$  ;

**return**  $\text{Bin}_{FD}(\text{Scale}(M(s, m, k)))$  vectors for each range of sample size;

**forall**  $s_i, s_j \in S_{i \neq j}$  **do**

$AMI(s_i, s_j)$ ;  
 Sum the AAMI values for each sample  $s_i$ , that are calculated between each vectors of size  $|K|$  for the given  $m$  for each sample;  
 Divide the Sum by the size of total range  $|S|$  for each  $s_i$  to find average adjusted mutual information of the given sample  $s_i$ .

**return**  $AMI(s_i)$

---

Figure 1. In the library step, we applied eight algorithms combined with the following different parameters: K-means, Agglomerative, Spectral, Birch, GaussianMixture, HDBSCAN, DBSCAN, and Affinity Propagation. Therefore, the complexity of the local step is the sum of the complexity of the algorithms (see Table 1). Once the Library step's clustering results are produced, their resulting clusters are found by applying four different consensus functions at the consensus step. The final consensus function is selected as the one that gives the maximum AAMI result among four different functions. For the final step of Strategy 1, the best match is selected by the maximum AMI result given between the consensus function and the hyperparameter set of ensembles.

Algorithm	Time Complexity	Category
K-means	$\mathcal{O}(kNT)$	Partitioning
Agglomerative	$\mathcal{O}(N^2)$	Hierarchical
Spectral	$\mathcal{O}(N^3)$	Model-Based
HDBSCAN	$\mathcal{O}(N \log N)$	Density-Based
DBSCAN	$\mathcal{O}(N \log N) \mid \mathcal{O}(N^2)$	Density-Based
Birch	$\mathcal{O}(N)$	Hierarchical
GaussianMixture	$\mathcal{O}(N^2KD)$	Distribution
AffinityPropagation	$\mathcal{O}(N^2 \log N)$	Model-Based

**Table 1**

N: Number of samples, k: number of clusters, T: number of iterations, D: dimension

For the first step of Strategy 2, we consider clustering to be obtained with the consensus function. As explained in Section 3, the higher the variance, the more accurate the results that can be extracted. To this end, a new ensemble set is obtained by sorting AAMI values from low to high and then eliminating those above a particular threshold value to reduce redundancy and complexity. Thus, clusters that produce similar labels are removed from the ensemble, and clustering is obtained with the consensus function among the remaining clusters. As shown in Figure 6, when the AAMI scores of the relevant approach are sorted and observed according to the number of algorithms in the entire ensembles, it is revealed that both approaches have different threshold values. Regarding N2d, these values show similar patterns in 10- or 2-dimensional representations, which is stabilized earlier than nearly half the value for UMAP. Considering that the AAMI results of different approaches have different distributions, threshold values of 100 and 200 are set for N2d and UMAP, respectively. After that, all steps in Strategy 1 are applied to this new set. As a result, labels are obtained with six different clustering approaches for each dataset.

## 5.4. Evaluation

### 5.4.1. Clustering Results

The primary purpose of clustering validation is to discriminate among reading behaviour groups, which would



## Unsupervised Behaviour Analysis of News Consumption in Turkish Media

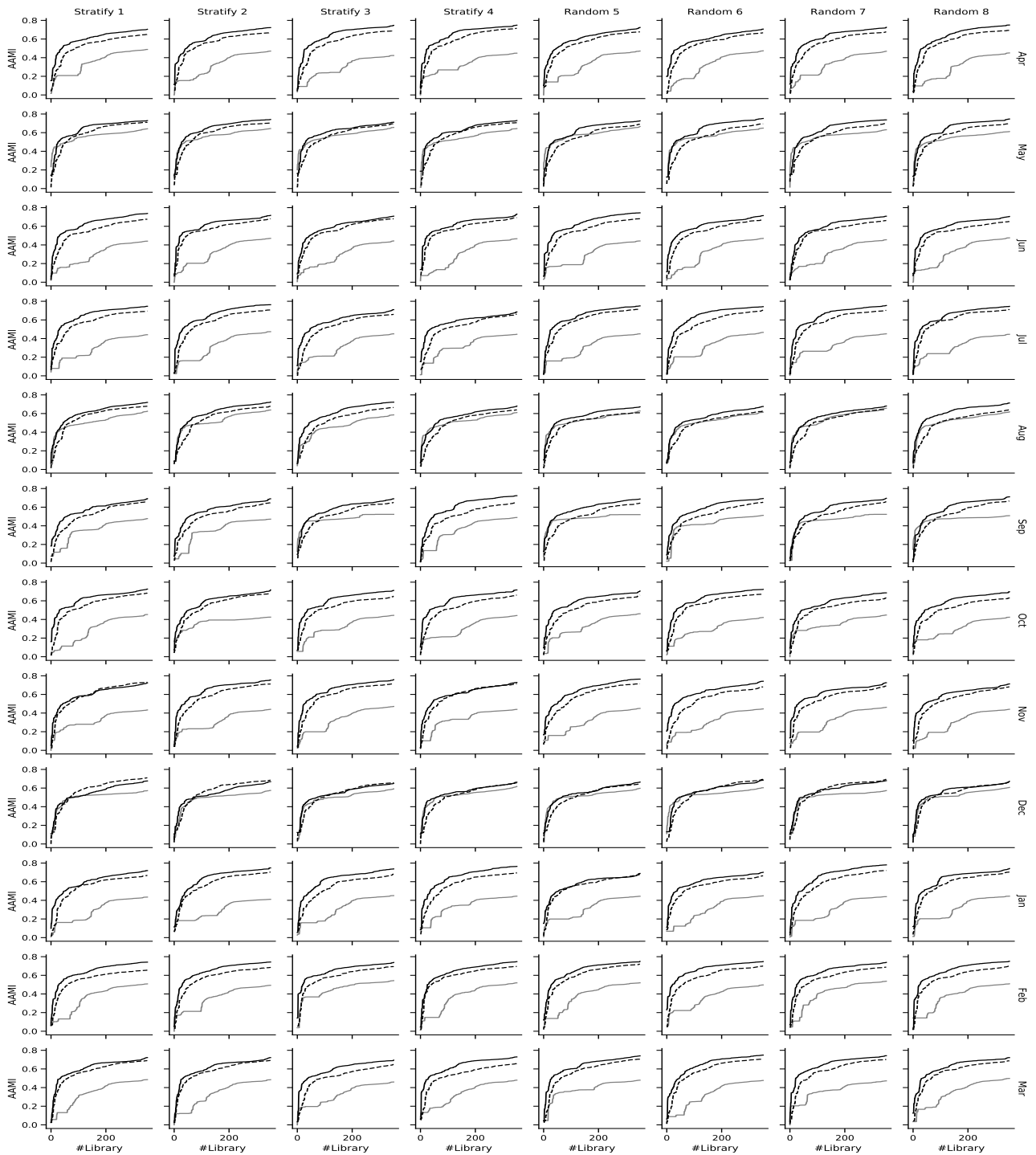


**Figure 6:** AAMI results are obtained after the decreased ensemble approach. The colours in the graph lines represent applied embeddings that are UMAP, 10-dimensional N2d, and 2-dimensional N2d given in grey, dashed black, and black, respectively. The rows represent months, and the columns represent the sampling strategy with index numbers. Each chart includes the number of clustering configurations on the X-axis, while the Y-axis shows the total selections.

help newsrooms recommend specific news for those in the given clusters. Since we have 6 different strategies with all consensus clustering labels, there are 356 possible clustering solutions in total. Therefore, the evaluation of the resulting clustering is nontrivial for this study since there is no ground truth available in the data and the knowledge-based inter-

pretations are subjective. Consequently, in the first step, we aimed to reach the best evaluation results among the clustering approaches. To identify successful strategies, internal validation metrics (SI, CH, DB, S-Dbw (Kim and Lee, 2003; Tong and Tan, 2009; Halkidi and Vazirgiannis, 2001) (see Appendix A.1) are compared based on the results of

**Table 2**  
Evaluated metrics' comparison

Metric	#Cluster Bias	Handling Noise	Sub Clusters	Skew Distribution	Optimal Value
SI	No	Depends on Noise(%)	No	Yes	Max
CHI	No	No	Yes	No	Max
DB	No	Yes	No	Yes	Min
S-Dbw (Halkidi)	Yes	Yes	Yes	Yes	Min
S-Dbw (Kim)	Yes	Yes	Yes	Yes	Min
S-Dbw (Tong)	No	Yes	Yes	Yes	Min

S-Dbw (Halkidi) (Halkidi and Vazirgiannis, 2001), S-Dbw (Kim) (Kim and Lee, 2003), S-Dbw (Tong) (Tong and Tan, 2009)

the clustering algorithms obtained for the month, embedding and sampled dataset. With this, we could observe both compactness/separation and arbitrary shape density validation of the clusters. As stated in a previous study (Handl et al., 2005), internal validation metrics must be selected by the applied clustering algorithms since both of them consider the underlying structure of the given dataset. Therefore, the metrics, especially when the ground truth is not known, are crucial for validating the resulting clusters. As reviewed in the study (Wegmann et al., 2021), metrics also come from certain assumptions, so there is a trade-off in the choice of these evaluations. In the given review study, cluster validation evaluated four main categories: Cluster (shape (spherical/convex, nonstandard geometry, arbitrary) and numbers (can be attributed to the high number of clusters)), Handling Noise (ability to deal with outliers without preprocessing) and Computational cost/complexity. On the other hand, capability with subcluster identification and skew distribution were also evaluated by another study (Liu et al., 2010b) (See Table 2).

Therefore, we evaluated cluster performances in a format that included various validation perspectives, as different characteristics of clusters could be focused on. Internal validation values are used as a measure to determine the optimality as the quality of clusters, which gives successful results in a previous study on identifying behaviours (Rodríguez-Fernández et al., 2017). Following this purpose, internal validation metrics of the clusters formed by the algorithms within the ensemble groups created separately by Strategies 1 and 2 are evaluated. Considering the optimal value of the metrics at the minimum and maximum limits, all scores are unit-based scaled between  $[0,1]$  within the evaluated dataset. Then, the successful metric was determined according to the one with the highest variance among these lists. As shown in Fig 7, although there are standard metrics, the majority of the selection belongs to CHI(%76) among all, and the rest

of the top selections are S-Dbw (Kim and Lee, 2003)(%8), SI(%7), S-Dbw (Halkidi and Vazirgiannis, 2001)(%5) and S-Dbw (Tong and Tan, 2009)(%4). The algorithm classes that take the best values in the limits of the metrics with the maximum variance are shown in Fig 8. According to the results, while the most successful algorithm for CHI is K-means, HDBSCAN did not give any results with CHI, which obtains the best validation scores with S-Dbw. Therefore, this result also supports the internal validation approach of S-Dbw, which considers the density area in the selected cluster.

#### 5.4.2. Selection of Successful Strategy

To select the most successful embedding and strategy, we utilize the closeness of the strategies and embedding approaches to the optimal metric scores. Although the CHI metric is found to give a generalizable result, it has been observed that different metrics can give optimal results in some months due to the differences in the distributions of the monthly dataset samples. For this reason, the metric values obtained with the strategies and approaches are evaluated with the filtering approach described in Table 3.

1. First, the algorithms, which are given by the metrics obtained according to the maximum variance calculation, are extracted (Optimal/Metric). Then, considering the optimal value of the metrics at the minimum and maximum limits for each breakdown, the top 5 results with the best score are obtained and ranked between 1 (the best) and 5 (the least). Thus, optimal metrics giving the best five scores for Strategy 1 and Strategy 2 and algorithms providing these metrics (Optimal/Algorithm) are prepared.
2. The closeness of the applied strategies' metric scores is calculated by taking the differences of the optimal metric values, which can be selected differently from CHI according to the datasets, and the corresponding metric values of the applied strategies on that dataset. The value differences are then scaled within the observed metrics between  $[0,1]$ ; 0 represents the closest to the optimal value, while 1 represents the farthest (Evaluation/Closeness). 1 is the closest to the optimal value.
3. The top 5 optimal algorithms filtered in the first step are compared with the algorithms obtained with the strategies, and their performances are weighted with specific coefficients. These coefficients are determined so that if an exact match with the algorithm (including all hyperparameters) occurs (Evaluation/Exact Match), the optimal algorithm's rank is (1-5), and if not, the minimum value (6) is placed (Evaluation/Rank Weighted). We evaluated the closeness of the clusters formed by the consensus function to the optimal algorithm with the ranking value obtained by the hyperparameter match method, since there can be no match with any optimal algorithm in the consensus step. Because the clusters are obtained as a result of consensus, the algorithm with the highest similarity

## Unsupervised Behaviour Analysis of News Consumption in Turkish Media

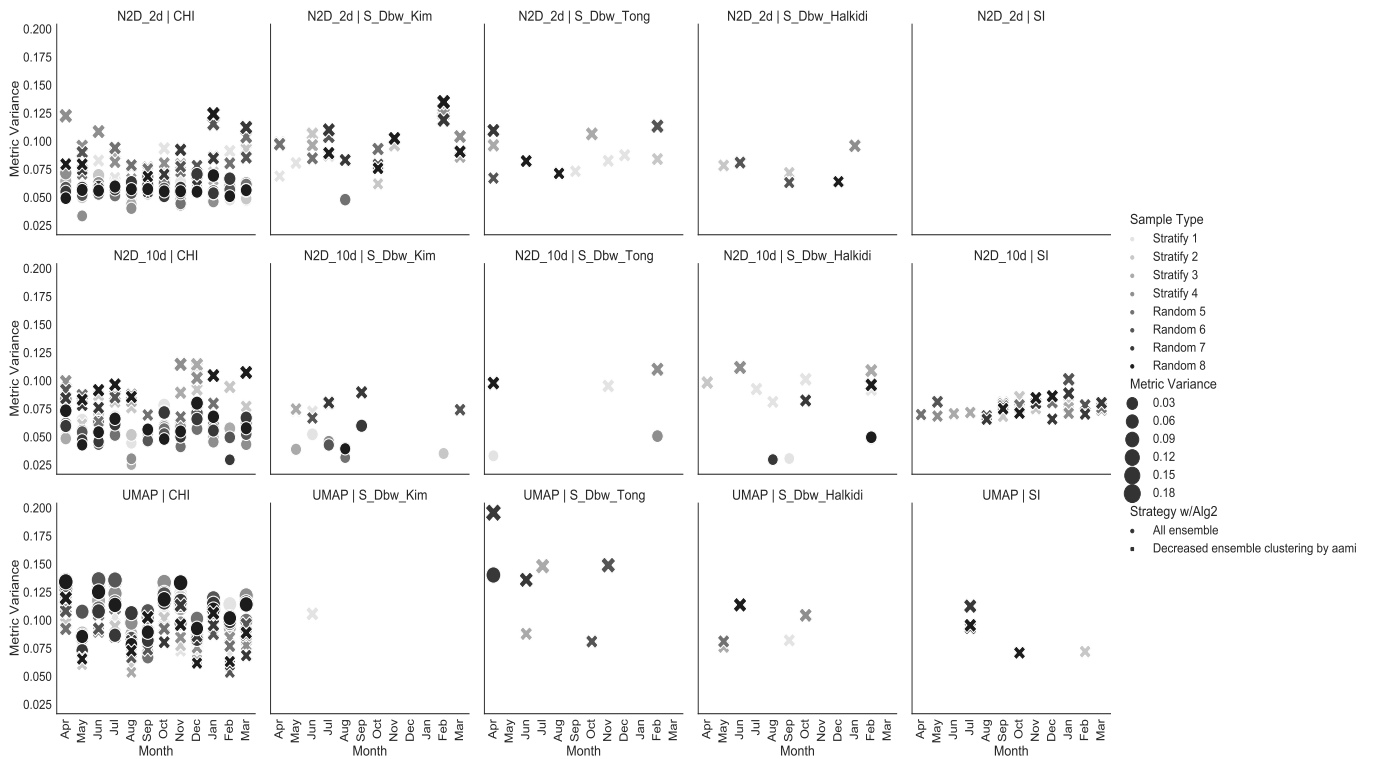


**Figure 7:** Metric selection by individual datasets sampled from each month and applying different strategies to embeddings. The cross sign "x" represents the optimal library metric results according to the decreased ensemble library, and sphere "o" represents the entire ensemble set.

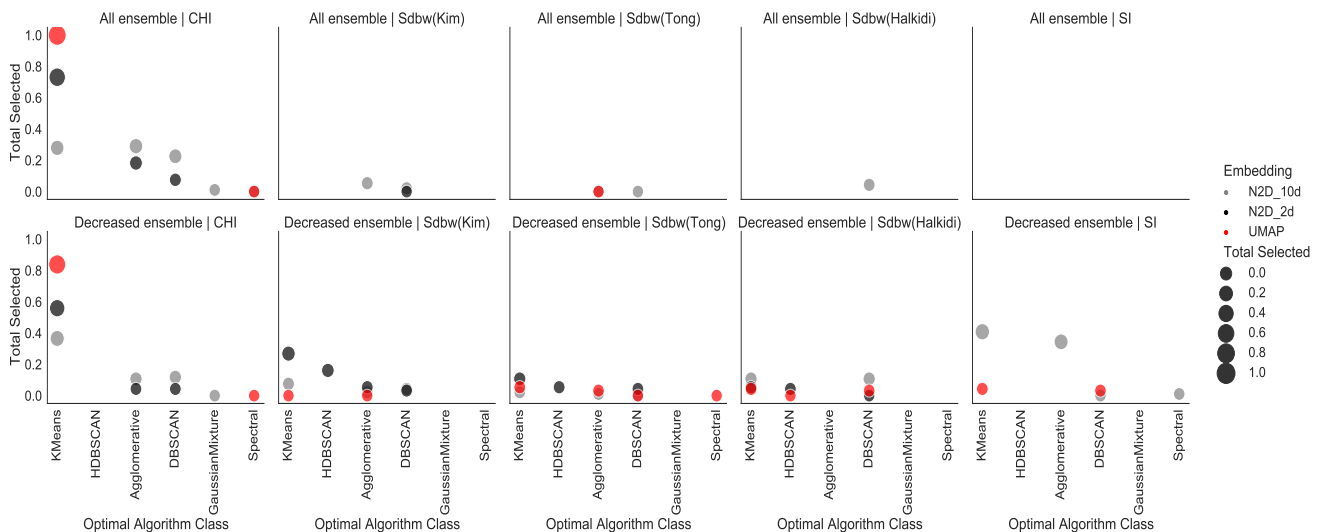


**Figure 8:** Optimal metrics obtained according to the maximum variance selection and algorithms that take their values at the maximum limits of these metrics. While the columns show the selected metrics, each strategy groups are represented in the rows. Embedding breakdowns are discriminated by the colors, where gray, black and red represent N2d-10d, N2d-2d, and UMAP, respectively. The area size of the circles scales the total number of selections.

to the library is found by the hyperparameter match method. Therefore, this similarity gives us the similarity of the consensus result to the optimal values (Evaluation/Rank Weighted, in red). However, we observed that the internal validation scores of the optimal algorithms on the samples give more successful

results than the clusters obtained by consensus.

4. The scaled closeness values, which are obtained in the second step, are multiplied by the coefficients obtained in the third step (Evaluation/Rank Weighted \* Evaluation/Closeness = Evaluation/Weights). Then, based on each sample, the results are ranked between

1 (the best) and 6 (the farthest) (Evaluation/Rank). Therefore, considering the entire dataset, the embedding approach with the highest number of times ranked 1 is the closest to the optimal value.

The successful strategy is found by following the applied embedding considering the ranking criterion given in the Evaluation/Rank column (Table 3). Thus, the results are ranked from minimum values to give the closest result to the optimal value and the maximum values to give the farthest result. At the same time, the performances of strategies that can achieve one-to-one matches were also weighted. In this step, we also discriminate the rankings as stratified and randomized to compare the sampling types.

As illustrated in Fig 9, even though there are ranked one results and one-to-one matching algorithms with optimal algorithms of N2d-10d and N2d-2d embeddings, the closest approach to the optimal algorithm is Hyperparameter Match Strategy 1 with UMAP embedding, which has the highest number of selections in rank 1. Based on these results, we conclude that Hyperparameter Match Strategy 1 with the UMAP result is the closest approach to the optimal values. Additionally, we conclude that the CHI metric produces the best quality clusters compared to other metrics. When we compare sample types, we can say that stratifying and random sampling mostly show similar behaviours, which may be due to the solid semantic correlation of the datasets within months.

### 5.4.3. Cluster Stability

The stability of the clusters is defined as the reoccurrence of the resulting clusters in different periods, even when the data points change. Some previous studies applied this procedure by having frequent samples without replacements and averaging the similarities with the Jaccard coefficient (Grech and Clough, 2016b). Another study investigated this approach to compare similarity between monthly samples of a digital library (Bogaard et al., 2019b) which concluded that there is a trade-off between silhouette width and the stability scores of the clusters. Our study validates the stability of resulting clusters in separated months by computing the average AMI scores to indicate clustering quality, which also means that these clusters are the general reading behaviours of the users whose referral channels are Twitter.

**Cluster Distributions:** To determine the stability, for each cluster,  $C_i$ , the distribution of the categorized and binned feature values,  $f_k$ , of  $n$  dimensional feature set,  $F_i^j = \{F_i^1, F_i^2, \dots, F_i^n\}$ , is obtained in each sample as follows:

$$F_i^j = \left( \frac{f_1}{C_i}, \frac{f_2}{C_i}, \dots, \frac{f_k}{C_i} \right), \quad C_i = \sum_k f_k, \quad (2)$$

where  $F_i^j$  represents the  $j^{\text{th}}$  feature of the  $i^{\text{th}}$  cluster, and the size of the cluster  $C_i$  is defined by the total size of features,  $f_k$ .

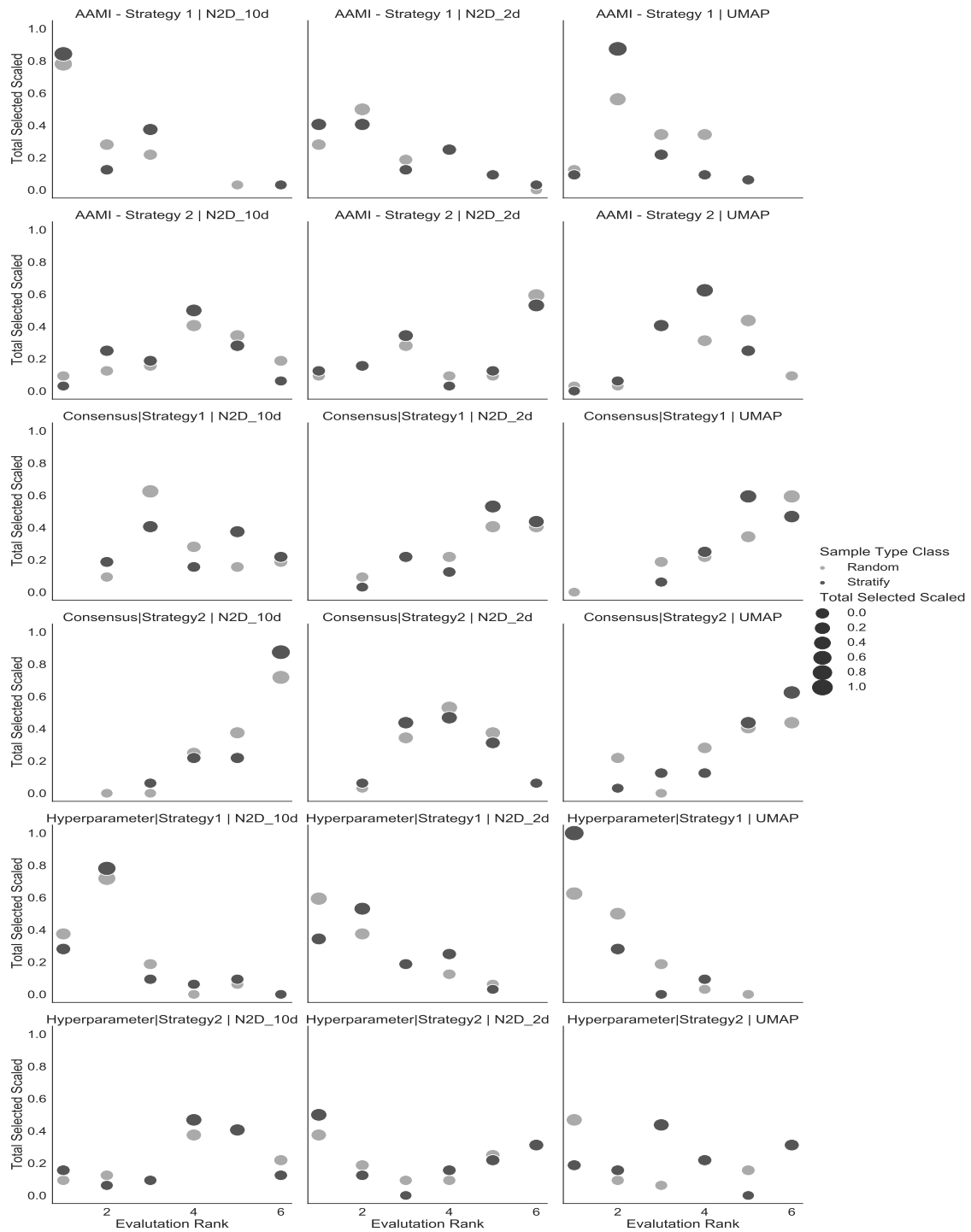
Fig 10 shows, per cluster, that have more than 0.5 AMI values according to 2 when compared with the rest of the

Table 3: Clusters with the highest reoccurrence counts

Month / Sample	Strategy, Dataset, Approach			Optimal			Selected			Evaluation					
	Embedding	Strategy w/Alg	Strategy	Class	Hyper-parameters	Metric Value	#Clusters	Hyper-parameters	Class	#Clusters	Exact Match	Closeness	Rank Weighted	Weights	Rank
N2d_10d		DE	CC-Stg 2	Agg	L2_Avg_2	SI - 0.662	2	hgpa k = 4	HGPA	163	0	0.56	6	3.34	6
			HM - Stg 2	Agg	L2_Avg_2	SI - 0.662	2	Euc_comp_14	K-means	4	0	0.32	6	1.93	5
May / Random 6		AE	CC-Stg 1	K-means	k = 30	CHI - 8459,528	30	hgpa L1_15_0.8	HGPA	290	0	0.23	6	1.40	4
			HM - Stg 1	K-means	k = 30	CHI - 8459,528	30	Euc_avg_26	DBSCAN	68	0	0.21	6	1.28	3
UMAP		DE	CC-Stg 2	K-means	k = 30	CHI - 13293,156	30	hgpa L1_Avg_10	HGPA	163	0	0.37	6	2.20	5
			HM - Stg 2	K-means	k = 30	CHI - 13293,156	30	Euc_avg_10	HDBSCAN	63	0	0.37	6	2.24	6
		AE	CC-Stg 1	K-means	k = 30	CHI - 13293,156	30	hgpa Birch_30	HGPA	250	0	0.34	6	2.04	4
			HM - Stg 1	K-means	k = 30	CHI - 13293,156	30	Euc_avg_24	Birch	30	0	0.13	6	0.77	1
N2d_2d		DE	CC-Stg 2	K-means	k = 30	CHI - 9998,848	30	hgpa L2_15_10	HGPA	163	0	0.27	6	1.63	5
			HM - Stg 2	K-means	k = 30	CHI - 9998,848	30	L2_20_20	HDBSCAN	112	0	0.27	6	1.62	4
		AE	CC-Stg 1	K-means	k = 30	CHI - 9998,848	30	hgpa Agg_ward_30	HGPA	276	0	0.28	2	0.55	2
			HM - Stg 1	K-means	k = 30	CHI - 9998,848	30	Agg_euc_avr_28	Agg	30	1	0.00	2	0.00	1
			ANMI - Stg 1	K-means	k = 30	CHI - 9998,848	30	Agg_euc_avr_28	Agg	28	0	0.15	6	0.88	3

Abbreviations used in the table: Strategy/Alg Decreased Ensemble: DA, All Ensemble: AE, Consensus Clustering: CC, Hyperparameter Match: HM, Averaged Normalized Mutual Information: ANMI, Strategy: Sig, Hyper-parameters: Complete: comp, Average: avg, Euclidean: Euc, Class: Agglomerative: Agg

## Unsupervised Behaviour Analysis of News Consumption in Turkish Media



**Figure 9:** Closeness of the metric scores obtained with the applied strategies to the optimal metric scores selected individually for the sampled dataset and ranked according to the filtering approach. Each embedding is represented in columns as N2d-10d, N2d-2d, and UMAP. While the columns show the embeddings, each strategy applied is represented in the rows. Stratify and random sample type breakdowns are discriminated in black and grey colours, respectively. Each chart includes rankings from 1 to 6 on the X-axis, while the Y-axis shows the total selections of these rankings during the year. The choice closest to the optimal metric value shows the approach and strategy with the highest total selection value in the 1<sup>st</sup> rank in this chart.

clusters in all months that are labelled as high stability. Since NER attributes are mostly related to the given text of articles, they are compared by including and excluding these features. The results show that the highest stability counts can be ob-

tained without NER attributes with an average stability of 10 out of 12 months. For example, in the Hyperparameter Match strategy, while 1 cluster obtained from April has matching clusters in June with NER included, the results in-

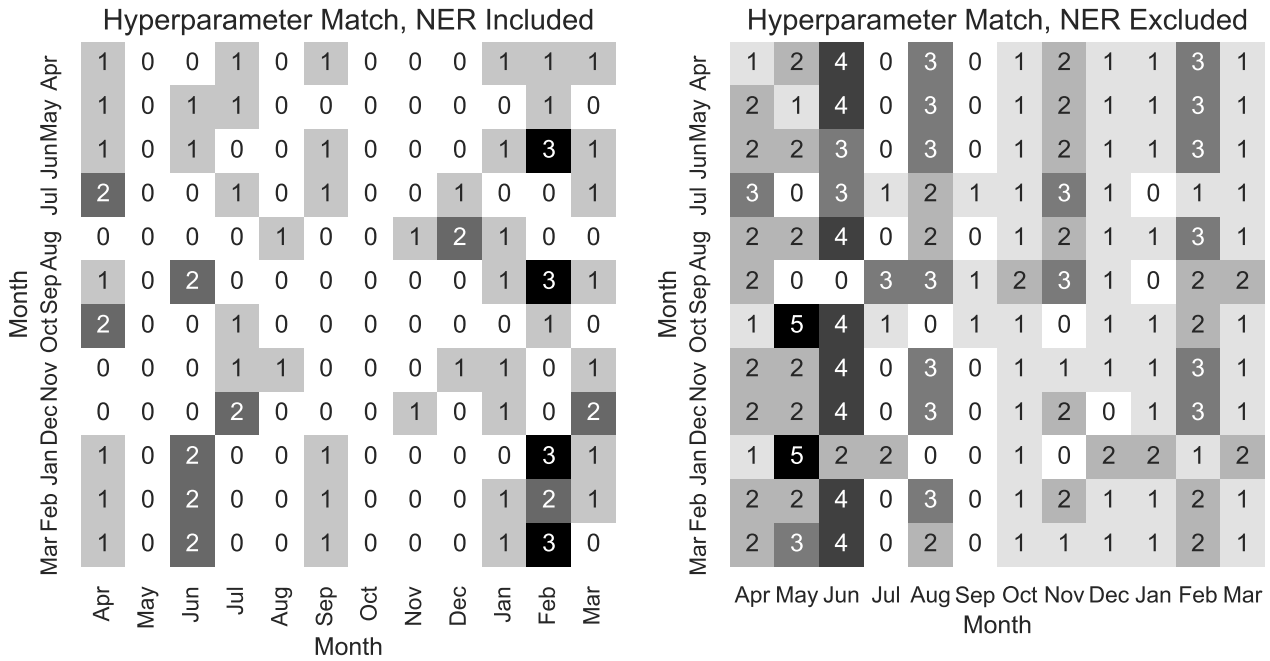


**Figure 10:** Comparison of all feature distributions over all clusters with AMI. The left figure includes the NER results, which are excluded from the right figure.

crease to 4 when NER results are excluded.

Table 4 represents the characteristics of the clusters related to the specific month, which reoccurred at the highest rate in other months. The observations from these clusters can be summarized as follows:

- In particular, the recently published articles that bounced from the first news item referred to in *City1* are stable for all clusters.
- The clusters with the highest volume did not achieve the similarity threshold with any clusters; instead, when we observe over months, the stability of the results is high, with a minimum rank of 4 and a maximum of 20 among all clusters.
- The entertainment category is primarily read in the afternoon with mobile devices.
- While weekday readers continue reading steadily over the months, the weekend readerships do not have high stability rates.
- The clusters that have columnists have higher ranked articles than other categories.
- While mobile users are often the greatest among device selection, PC users mostly read current affairs with political issues.

## 6. Conclusions and Future Work

Based on detailed clickstream data, this study reveals the reading patterns of anonymous readers whose referral channel is Twitter. Reading characteristics are first analysed by

the *leadcategory* distribution over months by location and device breakdowns, demonstrating that the underlying distribution diverges over time. An ensemble clustering analysis is utilized by comparing different embedding approaches and strategies on methodologically selected samples to identify stable clusters independent of time. Since the methodologies are applied based on the data from one news outlet, *Hürriyet*, the results may not be generalizable; thus, we conduct the stability analysis over months, which yields profoundly stable patterns. The promising characteristics of these findings show that some columnists have a substantial and continuous impact on delivering readers to a website. Mostly low ranked news is found to be directed, but in regard to the columnists and rarely directed locations, the behaviours change mainly to the high ranked contents. In general, morning readers are the majority, but entertainment news is mostly read in the afternoon. The latest generated news is preferred primarily by the readers, with which we can deduce that the readers are most interested in trending news.

Our empirical analyses with a comprehensive perspective of the clustering methodologies could find stable reading habits, leading to a number of further investigations. Our first plan is to reduce the complexity and increase the robustness of the experimental study on the decreased ensemble sets that we conducted, which can be improved by an iterative approach to find the optimal thresholds. We plan to incorporate sequential article data on news consumption, which is absent in our methodologies and could be insufficient to find the impacts of consecutive reading behaviours. Since our study focus does not fully reveal the underlying

**Table 4**  
Clusters with the highest reoccurrence count for a specific month

Month	Apr	May	Jun	Jul	Aug	Sep	Oct	Nov	Dec	Jan	Feb	Mar
Cluster Size(%) Rank	4,36 - 6	2,84 - 20	5,87 - 4	2,4 - 19	3,98 - 12	2,19 - 20	4,38 - 10	4,4 - 9	4,35 - 11	5,69 - 4	2,42 - 24	4,33 - 8
#of Reoccurrences Unique Months	19 - 10	19 - 10	19 - 10	17 - 10	19 - 10	19 - 9	18 - 10	19 - 10	19 - 9	18 - 9	19 - 10	18 - 10
Algorithm - #of Clusters	B - 30	B - 26	A - 30	B - 30	B - 30	A - 30	A - 30	A - 30	B - 20	A - 30	A - 30	A - 30
Bounce(%)	86.7	97.18	93.9	94.17	95.98	92.66	89.55	80	73.73	55.48	90.91	96.77
City1(%)	44.95	44.37	41.69	47.5	46.73	43.12	48.18	40.91	47.93	48.76	41.32	45.62
Recently Published (%)	97.25	93.66	99.66	98.33	95.98	95.41	86.82	98.64	98.62	98.23	28.1	60.37
Ranking(%)	LR - 78,9	LR - 40,14	MR - 68,47	MR - 31,67	LR - 43,72	LR - 41,28	LR - 45,45	LR - 41,82	LR - 36,41	LR - 33,22	LR - 97,52	LR - 97,24
Category(%)	CA - 63,3	E - 71,13	C - 56,95	C - 35	Et - 91,46	CA - 59,63	CA - 29,09	Et - 32,27	CA - 89,86	CA - 79,86	Et - 33,88	T - 38,71
Device(%)	M - 59,63	M - 97,89	M - 70,85	M - 75,83	M - 85,43	M - 82,57	M - 57,73	PC - 76,82	PC - 94,01	PC - 78,8	M - 87,6	M - 82,49
Hour(%)	AN - 9,63	AN - 11,27	MR - 13,22	MR - 21,67	AN - 13,07	AN - 17,43	MR - 14,09	AN - 14,09	MR - 12,9	AN - 14,84	AN - 10,74	MR - 15,67
NER(%)	IP - 17,4	UNK - 46,71	P - 26,44	P - 13,33	EtS - 63,82	UNK - 42,81	None - 21,6	UNK - 22,12	UNK - 10,6	P - 13,07	IP - 18,18	UNK - 59,44
Weekday(%)	39.45	42.25	26.1	49.17	26.63	56.88	25.45	34.09	23.5	80.21	40.5	39.63
Weeknumber(%)	1 <sup>st</sup> - 78,44	3 <sup>rd</sup> - 78,17	2 <sup>nd</sup> - 98,64	3 <sup>rd</sup> - 58,33	4 <sup>th</sup> - 100,0	4 <sup>th</sup> - 96,33	2 <sup>nd</sup> - 46,82	2 <sup>nd</sup> - 33,18	4 <sup>th</sup> - 96,31	4 <sup>th</sup> - 50,18	3 <sup>rd</sup> - 70,25	2 <sup>nd</sup> - 60,37

Abbreviations used in the table: *Algorithms* Agglomerative: A; Birch: B; Rank Low Rank: LR; Mid Rank: MR; *Category* Current Affairs: CA; Economy: E; Entertainment: Et; Travel: T; Columnist: C; *Device* Mobile: M; *Hour* Afternoon: AN; Morning: MR; *NER* City1 - Politics: IP; Unknown: UNK; Politics : P; Entertainment show: EtS

mechanism of these referral effects, future work based on social media with a holistic view may broadly expose these channels' reading characteristics. To enrich the semantics of future work, we plan to study transformer-based networks to explore the success of clickstream data embeddings on news outlet readership.

## A.1. Clustering Problem

The main goal of the clustering problem is to include similar data points in the same cluster and include different data points in separated clusters (Jain et al., 1999). According to this definition, we can define the clustering problem as follows in order to get the optimal result: Given set of data with  $n$  data points in  $d$  dimensions  $D = \{x_1, x_2, \dots, x_n\} \subseteq R^d$  we are in search of  $k$  number of clusters  $C = \{c_1, c_2, \dots, c_k\}$  whose intersection sets are empty and represents the partitions of primary data set. As a result, each data point is expressed with a label. When comparing clusters, one of the essential consideration is that labels obtained from different clustering algorithms can give the same similarity result for data points included in the same cluster, even if they come in different permutations. Because the purpose here is to compare whether the same data points are in the same cluster or different clusters. When we observe the labels obtained from two different clustering algorithms, such as  $K$  and  $K'$ , we aim to return the similarity ratio between  $[1,1,2,3,3]$  and  $[3,3,1,2,2]$  to be the maximum AMI value

## B.2. Internal Validation Metrics

**Silhouette coefficient (SI):** This metric gives results between  $[-1,1]$ , that is, the similarity of the data points within the cluster,  $a(i)$ , compared to other clusters,  $b(i)$ , where  $d(i,j)$  is the distance metric. Higher values indicate appropriate clusters.

$$a(i) = \frac{1}{|C_i| - 1} \sum_{j \in C, i \neq j} d(i, j)$$

$$b(i) = \min_{k \neq j} \frac{1}{|C_k|} \sum_{j \in C_k} d(i, j)$$

$$SI = \frac{1}{|D|} \sum_{i \in D} \frac{b(i) - a(i)}{\max\{a(i), b(i)\}} \quad (3)$$

**Dunn index-type (DI):** The value is a given ratio of inter-cluster distances over intra-cluster diameters, where higher values indicate better clusters. Out of several approaches to define the diameter of the cluster, in this study, we used the mean of pairwise distances in the cluster. Assuming  $x$  and  $y$  are the data points assigned in the same cluster from the given dataset  $D$  in  $n$  dimensions and there are  $k$  clusters, pairwise distances mean calculated as follows:

$$\mu = \frac{\sum_{x \in C_i} x}{|C_i|}, D_m = \frac{\sum_{x \in C_i} d(x, \mu)}{|C_i|}$$

$$DI_k = \frac{\min_{1 \leq i \leq j \leq k} \delta(C_i, C_j)}{\max_{1 \leq l \leq k} D_l} \quad (4)$$

**Calinski Harabasz index (CHI):** This index aims to find the ratio between cluster variance over within cluster variance, which is in the range of  $[0, \infty)$ . Higher values indicate good clustering.

$$CHI = \frac{\frac{1}{k-1} \sum_{i=1}^k \|\mu_i - \mu\|^2}{\frac{1}{|D|-1} \sum_{i=1}^k \sum_{x \in C_i} \|x - \mu\|^2} \quad (5)$$

**Davies Bouldin scores (DB):** This score gives how similar each cluster ( $C_i$ ) is to its most similar cluster ( $C_j$ ) on average. It measures intra- and inter-cluster distance ratios. The lower values indicate appropriate clustering where it ranges between  $[0, \infty)$ . When the average distance between each data point and the centre of the cluster is defined as  $S_i$  and the inter-cluster centroid distance is defined as  $N_{i,j}$ , the measurement of the goodness of the cluster,  $R_{i,j}$ , and the Davies-Bouldin index is defined as follows:

$$R_{i,j} = \frac{S_i + S_j}{N_{i,j}}$$

$$DB = \frac{1}{k} \sum_{i=1}^k \max_{i \neq j} R_{i,j} \quad (6)$$

**Scatter and Density between clusters (S-Dbw) Validity Index:** This metric consists of two objectives, as shown below. The first part  $Scat(\#c)$  is related to the average scattering within the clusters that is obtained by partitioning the dataset. Therefore, minimum values indicate better results in terms of compactness and separation. The second part  $Dens\_bw(\#c)$  considers intra-cluster densities by comparing the clusters' centre points; thus, minimum values also indicate better separation.

$$Scat(\#c) = \frac{\frac{1}{\#c} \sum_{i=1}^{\#c} \|\sigma(C_i)\|}{\|\sigma(D)\|}$$

$$Dens\_bw(\#c) = \frac{1}{\#c(\#c-1)} \sum_{i=1}^{\#c} \left[ \frac{\sum_{x \in C_i \cup C_j} f(x, u_{i,j})}{\max\{\sum_{x \in C_i} f(x, c_i), \sum_{x \in C_j} f(x, c_j)\}} \right]$$



$$S - Dbw = Scat(\#c) + Dens\_bw(\#c) \quad (7)$$

(#c: Number of total clusters,  $C_i$ : i-th cluster,  $\sigma(C_i)$ : variance of  $C_i$ ,  $D$ : Dataset,  $f(x, u_{i,j})$ : the midpoint of the clusters' centers as a defined line segment,  $\|X\| = (X^T X)^{1/2}$ )

There are other versions on S-Dbw which we compare during the study. The problem with S-Dbw reflected by other studies. The first drawback is, since  $Dens\_bw(\#c)$  in S-Dbw measures neighborhood within the standard deviation, it could not cover the inter-cluster similarity especially for the non-circular clusters. Secondly,  $Scat(\#c)$  part for intra-cluster similarity does not take into account tuples which might effect when there is similar variance among two cluster with difference tuple sizes.

The approach introduced by Kim et. al. (Kim and Lee, 2003), for the second part of the formulation, uses cluster based inter-cluster similarity by considering confidence interval for each dimension which provides to be defined the size and shape of the densities of clusters, on the other hand for intra-cluster similarity uses weighted average variance within clusters.

Tong et. al (Tong and Tan, 2009) note some drawbacks introduced by (Kim and Lee, 2003). Since (Kim and Lee, 2003) does not consider the discrepancy among the clusters, selecting the middle point of the margin notoriously affects the centre choice.  $Scat(\#c)$  points out that when cluster numbers are increasing, the result of this part will be monotonically increasing as well. To overcome these, for the  $Dens\_bw(\#c)$  part, this approach selects the margin region instead of the middle point of the line segment among clusters to improve intercluster similarity. For intracluster similarity. Within-cluster similarity prevents monotonically increasing values by keeping the constant, although the number of clusters increases.

### C.3. External Validation Metrics

**Normalized Mutual Information (NMI):** In information theory, Mutual Information (MI) is defined as the amount of information obtained from one discrete-valued random variable  $X$ , by observing the other random variable  $Y$ . Assuming the joint probability distribution of two random variables is  $\rho_{X,Y}$  and the expected value of this distribution is  $E_\rho$ , then MI is defined as:

$$I(X, Y) = E_{\rho_{X,Y}} \left[ \log \frac{\rho_{X,Y}}{\rho_X \cdot \rho_Y} \right]$$

Since  $I(X, Y)$  is not bounded above, normalizing it provides

the results in the range of  $[0, 1]$ , assuming  $H(X)$  and  $H(Y)$  are the marginal entropies of random variables;

$$H(X) = -E_{\rho_X}[\log \rho_X], I(X, Y) \leq \min(H(X), H(Y))$$

$$NMI(X, Y) = \frac{I(X, Y)}{\sqrt{H(X)H(Y)}} \quad (8)$$

As defined in (Strehl and Ghosh, 2002), NMI can be interpreted as the label similarities of the clustering results, even though they might come from different permutations. In this case, the assumed  $X$  and  $Y$  discrete random variables can be interpreted as  $C$ , as clustered data label assignments, and  $C^*$  as ground-truth labels.

**Adjusted Mutual Information (AMI):** The adjustment of the result from MI is needed, since MI values are higher when there are a larger number of clusters not necessarily having more information shared among them. MI is adjusted for chance as follows (Vinh et al., 2010), which ranges between  $[0, 1]$  such that 1 indicates that two label assignments are equal:

$$AMI(C, C^*) = \frac{I() - E(I)}{\text{mean}(H(C), H(C^*)) - E(I)} \quad (9)$$

**Averaged Normalized Mutual Information:** As defined in (Helfmann et al., 2018), in a given ensemble of clusterings  $K$ , we can obtain the single clustering  $C$  information shared with the whole set of ensembles with the size of  $m$  by:

$$ANMI(C, K) = \frac{1}{m} \sum_{i=1}^m NMI(C, C_i) \quad (10)$$

### D.4. Distance Metrics

**Jensen-Shannon Divergence (JSD):** Symmetric results and finite values are given when computing probability vectors defined as considering  $U$  and  $V$  are the vectors of different distributions.  $D$  is the Kullback–Leibler divergence, and  $m$  is the mean of the vectors computed pointwise. Kullback–Leibler measures the distance between two vectors by calculating entropy, and each vector value is summed to 1:

$$JSD : \sqrt{\frac{D(u||m) + D(v||m)}{2}} \quad (11)$$

$$D_{KL}(U||M) = - \sum_{x \in X} U(x) \log \frac{M(x)}{U(x)} \quad (12)$$

(Menéndez et al., 1997)

## CRedit authorship contribution statement

**Didem Makaroğlu:** Conceptualization, Methodology, Software, Validation, Investigation, Data curation, Writing - original draft, Writing - review and editing, Visualization.  
**Altan Cakir:** Conceptualization of this study, supervising, review and editing.  
**Behçet Uğur Töreyn:** Conceptualization of this study, Methodology, review and editing.

## Acknowledgement

Authors would like to thank Demirören Teknoloji A.S. for the support and providing data.

## References

- Akbari, E., Dahlan, H.M., Ibrahim, R., Alizadeh, H., 2015. Hierarchical cluster ensemble selection. *Engineering Applications of Artificial Intelligence* 39, 146–156.
- Alizadeh, H., Minaei-Bidgoli, B., Parvin, H., 2014. To improve the quality of cluster ensembles by selecting a subset of base clusters. *Journal of Experimental & Theoretical Artificial Intelligence* 26, 127–150.
- Aras, G., Makaroğlu, D., Demir, S., Cakir, A., 2021. An evaluation of recent neural sequence tagging models in turkish named entity recognition. *Expert Systems with Applications* 182, 115049.
- Arora, P., Varshney, S., et al., 2016. Analysis of k-means and k-medoids algorithm for big data. *Procedia Computer Science* 78, 507–512.
- Azimi, J., Fern, X., 2009. Adaptive cluster ensemble selection, in: *Twenty-First International Joint Conference on Artificial Intelligence*.
- Banerjee, A., Dave, R.N., 2004. Validating clusters using the hopkins statistic, in: *2004 IEEE International conference on fuzzy systems (IEEE Cat. No. 04CH37542)*, IEEE. pp. 149–153.
- Bar-Gill, S., Inbar, Y., Reichman, S., 2021. The impact of social vs. non-social referring channels on online news consumption. *Management Science* 67, 2420–2447.
- Benlian, A., 2015. Web personalization cues and their differential effects on user assessments of website value. *Journal of management information systems* 32, 225–260.
- Bogaard, T., Hollink, L., Wielemaker, J., Hardman, L., Van Ossenbruggen, J., 2019a. Searching for old news: User interests and behavior within a national collection, in: *Proceedings of the 2019 Conference on Human Information Interaction and Retrieval*, pp. 113–121.
- Bogaard, T., Hollink, L., Wielemaker, J., Hardman, L., Van Ossenbruggen, J., 2019b. Searching for old news: User interests and behavior within a national collection, in: *Proceedings of the 2019 Conference on Human Information Interaction and Retrieval*, pp. 113–121.
- Boongoen, T., Lam-On, N., 2018. Cluster ensembles: A survey of approaches with recent extensions and applications. *Computer Science Review* 28, 1–25.
- Caliriński, T., Harabasz, J., 1974. A dendrite method for cluster analysis. *Communications in Statistics-theory and Methods* 3, 1–27.
- Castellano, G., Fanelli, A.M., Torsello, M.A., 2013. Web usage mining: discovering usage patterns for web applications, in: *Advanced Techniques in Web Intelligence-2*. Springer, pp. 75–104.
- Catledge, L.D., Pitkow, J.E., 1995. Characterizing browsing strategies in the world-wide web. *Computer Networks and ISDN systems* 27, 1065–1073.
- Chiou, L., Tucker, C., 2017. Content aggregation by platforms: The case of the news media. *Journal of Economics & Management Strategy* 26, 782–805.
- Dellarocas, C., Katona, Z., Rand, W., 2013. Media, aggregators, and the link economy: Strategic hyperlink formation in content networks. *Management science* 59, 2360–2379.
- Dunn, J.C., 1974. Well-separated clusters and optimal fuzzy partitions. *Journal of cybernetics* 4, 95–104.
- Fern, X.Z., Brodley, C.E., 2004. Solving cluster ensemble problems by bipartite graph partitioning, in: *Proceedings of the twenty-first international conference on Machine learning*, p. 36.
- Fern, X.Z., Lin, W., 2008. Cluster ensemble selection. *Statistical Analysis and Data Mining: The ASA Data Science Journal* 1, 128–141.
- Flaxman, S., Goel, S., Rao, J.M., 2016. Filter bubbles, echo chambers, and online news consumption. *Public opinion quarterly* 80, 298–320.
- Freedman, D., Diaconis, P., 1981. On the histogram as a density estimator: L<sub>2</sub> theory. *Zeitschrift für Wahrscheinlichkeitstheorie und verwandte Gebiete* 57, 453–476.
- Grech, D., Clough, P., 2016a. Investigating cluster stability when analyzing transaction logs, in: *Proceedings of the 16th ACM/IEEE-CS on Joint Conference on Digital Libraries*, pp. 115–118.
- Grech, D., Clough, P., 2016b. Investigating cluster stability when analyzing transaction logs, in: *Proceedings of the 16th ACM/IEEE-CS on Joint Conference on Digital Libraries*, pp. 115–118.
- Halkidi, M., Vazirgiannis, M., 2001. Clustering validity assessment: finding the optimal partitioning of a data set, in: *Proceedings 2001 IEEE International Conference on Data Mining*, pp. 187–194. doi:10.1109/ICDM.2001.989517.
- Handl, J., Knowles, J., Kell, D.B., 2005. Computational cluster validation in post-genomic data analysis. *Bioinformatics* 21, 3201–3212.
- Helfmann, L., von Lindheim, J., Mollenhauer, M., Banisch, R., 2018. On hyperparameter search in cluster ensembles. *arXiv preprint arXiv:1803.11008*.
- Jain, A.K., Murty, M.N., Flynn, P.J., 1999. Data clustering: a review. *ACM computing surveys (CSUR)* 31, 264–323.
- Jing, L., Tian, K., Huang, J.Z., 2015. Stratified feature sampling method for ensemble clustering of high dimensional data. *Pattern Recognition* 48, 3688–3702.
- Kim, Y., Lee, S., 2003. A clustering validity assessment index, in: *Pacific-Asia Conference on Knowledge Discovery and Data Mining*, Springer. pp. 602–608.
- Köster, A., Matt, C., Hess, T., 2021. Do all roads lead to rome? exploring the relationship between social referrals, referral propensity and stickiness to video-on-demand websites. *Business & Information Systems Engineering* 63, 349–366.
- Kuncheva, L.I., Vetrov, D.P., 2006. Evaluation of stability of k-means cluster ensembles with respect to random initialization. *IEEE transactions on pattern analysis and machine intelligence* 28, 1798–1808.
- Li, T., Ding, C., Jordan, M.I., 2007. Solving consensus and semi-supervised clustering problems using nonnegative matrix factorization, in: *Seventh IEEE International Conference on Data Mining (ICDM 2007)*, IEEE. pp. 577–582.
- Lin, C., Xie, R., Guan, X., Li, L., Li, T., 2014. Personalized news recommendation via implicit social experts. *Information Sciences* 254, 1–18.
- Liu, J., Dolan, P., Pedersen, E.R., 2010a. Personalized news recommendation based on click behavior, in: *Proceedings of the 15th international conference on Intelligent user interfaces*, pp. 31–40.
- Liu, Y., Li, Z., Xiong, H., Gao, X., Wu, J., 2010b. Understanding of internal clustering validation measures, in: *2010 IEEE international conference on data mining*, IEEE. pp. 911–916.
- Makaroğlu, D., Çakır, A., Kocabaş, K., 2019. Social media and clickstream analysis in turkish news with apache spark, in: *International Conference on Intelligent and Fuzzy Systems*, Springer. pp. 221–228.
- Mao, E., Zhang, J., 2015. What drives consumers to click on social media ads? the roles of content, media, and individual factors, in: *2015 48th Hawaii International Conference on System Sciences*, IEEE. pp. 3405–3413.
- McConville, R., Santos-Rodriguez, R., Piechocki, R.J., Craddock, I., 2021.

- N2d:(not too) deep clustering via clustering the local manifold of an autoencoded embedding, in: 2020 25th International Conference on Pattern Recognition (ICPR), IEEE, pp. 5145–5152.
- McInnes, L., Healy, J., Astels, S., 2017. hdbscan: Hierarchical density based clustering. *Journal of Open Source Software* 2, 205.
- McInnes, L., Healy, J., Melville, J., 2020. Umap: uniform manifold approximation and projection for dimension reduction .
- Menéndez, M., Pardo, J., Pardo, L., Pardo, M., 1997. The jensen-shannon divergence. *Journal of the Franklin Institute* 334, 307–318.
- Möller, J., van de Velde, R.N., Merten, L., Puschmann, C., 2020. Explaining online news engagement based on browsing behavior: Creatures of habit? *Social Science Computer Review* 38, 616–632.
- Pivadori, M., Stegmayer, G., Milone, D.H., 2016. Diversity control for improving the analysis of consensus clustering. *Information Sciences* 361, 120–134.
- Rodríguez-Fernández, V., Menéndez, H.D., Camacho, D., 2017. A study on performance metrics and clustering methods for analyzing behavior in uav operations. *Journal of Intelligent & Fuzzy Systems* 32, 1307–1319.
- Rousseeuw, P.J., 1987. Silhouettes: a graphical aid to the interpretation and validation of cluster analysis. *Journal of computational and applied mathematics* 20, 53–65.
- Schubert, E., Sander, J., Ester, M., Kriegel, H.P., Xu, X., 2017. Dbscan revisited, revisited: why and how you should (still) use dbscan. *ACM Transactions on Database Systems (TODS)* 42, 1–21.
- Strehl, A., Ghosh, J., 2002. Cluster ensembles—a knowledge reuse framework for combining multiple partitions. *Journal of machine learning research* 3, 583–617.
- Su, Q., Chen, L., 2015. A method for discovering clusters of e-commerce interest patterns using click-stream data. *electronic commerce research and applications* 14, 1–13.
- Thorson, K., Wells, C., 2016. Curated flows: A framework for mapping media exposure in the digital age. *Communication Theory* 26, 309–328.
- Tong, J., Tan, H., 2009. Clustering validity based on the improved s\_dbw\* index. *Journal of Electronics (China)* 26, 258–264.
- Varia, J., Mathew, S., et al., 2014. Overview of amazon web services. *Amazon Web Services* 105.
- Vinh, N.X., Epps, J., Bailey, J., 2010. Information theoretic measures for clusterings comparison: Variants, properties, normalization and correction for chance. *The Journal of Machine Learning Research* 11, 2837–2854.
- Wang, G., Konolige, T., Wilson, C., Wang, X., Zheng, H., Zhao, B.Y., 2013. You are how you click: Clickstream analysis for sybil detection, in: 22nd {USENIX} Security Symposium ({USENIX} Security 13), pp. 241–256.
- Wang, G., Zhang, X., Tang, S., Zheng, H., Zhao, B.Y., 2016. Unsupervised clickstream clustering for user behavior analysis, in: Proceedings of the 2016 CHI conference on human factors in computing systems, pp. 225–236.
- Wegmann, M., Zipperling, D., Hillenbrand, J., Fleischer, J., 2021. A review of systematic selection of clustering algorithms and their evaluation. *arXiv preprint arXiv:2106.12792* .
- Wells, C., Thorson, K., 2017. Combining big data and survey techniques to model effects of political content flows in facebook. *Social Science Computer Review* 35, 33–52.
- Xu, J., Forman, C., Kim, J.B., Van Ittersum, K., 2014. News media channels: Complements or substitutes? evidence from mobile phone usage. *Journal of Marketing* 78, 97–112.
- Yanatma, S., 2018. Reuters institute digital news report 2018–turkey supplementary report .
- Yang, F., Li, T., Zhou, Q., Xiao, H., 2017. Cluster ensemble selection with constraints. *Neurocomputing* 235, 59–70.
- Yeo, I.K., Johnson, R.A., 2000. A new family of power transformations to improve normality or symmetry. *Biometrika* 87, 954–959.
- Zhang, J., Kamps, J., 2010. Search log analysis of user stereotypes, information seeking behavior, and contextual evaluation, in: Proceedings of the third symposium on Information interaction in context, pp. 245–254.
- Zheng, L., Li, L., Hong, W., Li, T., 2013. Penetrate: Personalized news recommendation using ensemble hierarchical clustering. *Expert Systems with Applications* 40, 2127–2136.